JOURNAL OF GEOPHYSICAL RESEARCH, VOL. 100, NO. A11, PAGES 21,489–21,501, NOVEMBER 1, 1995

Ionospheric plasma response to HF radio waves operating at frequencies close to the third harmonic of the electron gyrofrequency

F. Honary

Lancaster Communication Research Center, SECaM, , Lancaster University, Lancaster, England

A. J. Stocker, T. R. Robinson and T. B. Jones

Department of Physicss and Astronomy, Leicester University, Leicester, England

P. Stubbe

Max-Planck-Institute für Aeronomie, Katlenburg,-Lindau, Germany

Abstract. Experimental results concerning European incoherent scatter observations of heater-induced electron temperature enhancements, anomalous absorption of low-power HF probe waves, and the spectrum of stimulated electromagnetic emission (SEE) in the sidebands of a high-power HF electromagnetic wave are presented. For the experiments reported in this paper, an *O* mode pump wave was transmitted vertically into the *F* region above Tromsø, Norway, while the injected frequency was varied in small steps around the third harmonic of the electron gyrofrequency. Systematic variations with pump frequency were observed in the data obtained from all three diagnostics. Measurements of anomalous absorption, the downshifted maximum (DM) spectral feature, and heater-induced electron temperature enhancements all exhibited broad minima as the heater frequency approached the third harmonic of the electron gyrofrequency. In addition, the signal strength of the HF probe wave measured during heater off periods is also reduced at these and higher heater frequencies. The experimental findings suggest that at heater frequencies in the vicinity of the third gyroharmonic, small-scale field-aligned irregularities are not excited, whereas very small scale irregularities, of the order of a few electron cyclotron radii, which are responsible for the production of fast electrons, may be generated. The observed reduction in the diagnostic signal strength is then attributed to the ionized patches produced by these energetic electrons.

1. Introduction

A number of nonlinear processes may be initiated when a powerful electromagnetic wave, with *O* mode polarization, is launched from the ground into the ionosphere. These include heating of the ionospheric plasma and the formation of field-aligned plasma irregularities on a wide range of spatial scales, ranging from a few meters to tens of kilometers across the geomagnetic field. The excitation of short-scale field-aligned irregularities (FAI) in the upper hybrid resonance region is of special importance, since these irregularities are responsible for the anomalous absorption of any other electromagnetic wave passing through the instability region and cause anomalous heating of the plasma [*Vas'kov and Gurevich*, 1975, 1977; *Graham and Fejer*, 1976; *Das and Fejer*, 1979; *Stubbe and Kopka*, 1980; *Kuo and Lee*, 1982; *Stubbe et al.*, 1982a; *Dysthe et al.*, 1983; *Jones et al.*, 1984, 1986; *Robinson*, 1988, 1989]. Furthermore, a powerful electromagnetic wave can generate secondary electromagnetic waves in the sidebands of the primary HF wave which can then exit the ionosphere and be detected on the ground. Such radiation was discovered a decade ago [*Thidé et al.*, 1982, 1983, 1989; *Stubbe et al.*, 1984; *Fejer et al.*, 1985] and has been termed stimulated electromagnetic emission (SEE).

Paper number 95JA02098.
0148-0227/95/95JA-02098$05.00

Previous experimental observations have revealed that strong changes in the character of the SEE spectra occur when the pump frequency approaches a multiple of the electron gyrofrequency [*Leyser et al.*, 1989, 1990, 1992, 1993; *Stubbe and Kopka*, 1990]. These findings led to a series of experiments [*Belyakova et al.*, 1991; *Lobachevsky et al.*, 1992; *Stocker et al.*, 1993; *Stubbe et al.*, 1994], in which the anomalous absorption and phase changes measured on low-power HF diagnostic were made together with SEE spectral measurements, while the injected frequency was changed in small steps around the third, fourth, and fifth harmonics of the electron gyrofrequency. These experiments indicate that at pump frequencies close to electron gyroharmonics, not only are the SEE spectral features strongly modified, but also the anomalous absorption is greatly reduced. Since the heating of the high-latitude *F* region plasma is believed to be due mainly to the anomalous absorption of the electromagnetic wave rather than to collisional absorption, which is the dominant heating process in the *D* and *E* regions, this finding prompted an investigation into the heating of the plasma for pump frequencies close to electron gyroharmonics.

In this paper, multidiagnostic observations of the modified ionosphere are reported in which the SEE spectral features, anomalous absorption of low-power electromagnetic waves, and plasma parameters (electron temperature, T_e, and electron density, N_e) are measured simultaneously while the pump frequency is varied in small steps around the third harmonic of the electron gyrofrequency ($3f_{ce}$)

2. Experimental Arrangement

The experiments reported in this paper were carried out in October 1992. The heater, which is located at Ramfjordmoen about 16 km to the southeast of Tromsø, Norway, has been described by *Stubbe et al.* [1982b]. For these experiments the heater transmitted vertically with an effective radiated power (ERP) of 220 MW and *O* mode polarization, while the frequency was changed in small steps around $3f_{ce}$ For each transmitted frequency a tuning time of 1-2 min was required, the heater was then operated continuously (CW) for 4-5 min, and finally this was followed by a cycle of 1 min off, 1 min on, before tuning to the next frequency. Each experiment began at a heater frequency 100-150 kHz below the expected value of $3f_{ce}$ and then progressed in steps of 10-20 kHz upward through the harmonic and beyond, covering a range of about 200-300 kHz. Given favorable ionospheric conditions, a second run was made, covering approximately the same frequency range, but in which the frequency was stepped downward through the harmonic. An ionosonde colocated with the heater provided ionograms and hence a real-time indication of ionospheric conditions.

Observations of the modified ionosphere were made with the following diagnostics:

Low-power HF transmitter and receiver system. This system, which consists of four transmitters and five receivers, is described in detail by *Stocker et al.* [1993]. Transmitters were located at a site approximately 50 km north of the heater's location. Two transmitters were kept at fixed frequencies, while the other two transmitted at fixed frequency offsets (60-70 kHz) from the heater, one above and one below the pump frequency. The corresponding HF receivers were deployed 45 km to the south of the heater. This geometry was chosen deliberately to ensure that the low-power HF probe waves were not affected by the *D* and *E* regions directly illuminated by the main lobe of the heater. Four of five receivers monitored the HF probe waves, while the fifth receiver was used to observe the ionospherically reflected heater signal. Both the real and imaginary components of the received signals were recorded, which enabled both phase and amplitude measurements to be obtained. The anomalous absorption of the diagnostic waves and the pump wave may be derived from these data [e.g., *Robinson*, 1989].

European Incoherent Scatter Radar (EISCAT). For the experiments discussed in this paper, the European incoherent scatter (EISCAT) UHF facility [*Rishbeth and Williams,* 1985; *Rishbeth and VanEyken*, 1993] was employed. This is a tristatic system with a monostatic antenna, colocated with the heater near Tromsø, capable of both transmission and reception and remote receivers at Kiruna, Sweden, and Sodankylä, Finland. The UHF system was operating in a modified form of the common program 1, version J (CP-1-J), in which the Tromsø antenna was pointed vertically instead of along the local magnetic field line. In the CP-1-J program, four pulse schemes are transmitted: long pulse, alternating code, and two power profiles. Pulses of 350 µs duration provide long pulse measurements with 22.5-km altitude resolution which extends over 21 range gates from approximately 140 to 600 km in altitude. An alternating code transmission scheme is employed for high height resolution observations. The pulse length for this scheme is 21 µs, affording an altitude resolution of 3.15 km at heights between 86 and 270 km. Two power profiles are obtained from pulses of 40 µs and 21 µs duration, yielding altitude resolutions of 4.5 and 3.15 km, respectively. The excitation of parametric instabilities and the possible contamination of the incoherent scatter spectra with the heater-induced ion-line overshoot [e.g., *Jones et al.*, 1986] mean that data with high time resolution (5-10 s integration) are required in studying the modification effects. For the alternating code data this requirement leads to a poorly defined ion-line spectrum, and hence the derived electron temperature and density values contain large errors. The EISCAT data presented in this paper were acquired from the long-pulse scheme (22.5-km altitude resolution) with 5-s time resolution.

HF receiver and Spectrum analyzer. This equipment was located at a site 17 km southeast of the heater. The spectrum analyzer was employed for the real-time recording of the SEE spectra [e.g., *Stubbe et al.*, 1994].

3. Observations

The anomalous absorption of low-power diagnostic waves propagating through the heated region occurs when they are scattered into Langmuir waves by heater-induced FAI. Under the conditions encountered during experiments reported in this paper, the amplitude of the diagnostic signal begins to decay within a few seconds (1-8 s) of the heater switch-on. The difference between the received diagnostic signal amplitude when the heater is on and when the heater is off determines the level of anomalous absorption. Therefore, for each heater frequency there is a corresponding anomalous absorption measurement, which can be obtained from [e.g., *Robinson*, 1989]

$$\Gamma = A_{\rm off} - A_{\rm on} \tag{1}$$

where $A_{\rm off}$ and $A_{\rm on}$ correspond to the averaged signal strengths during the 1 min off, 1 min on part of the heater cycle, respectively. Since the anomalous absorption measured on a probe signal depends in part on the separation between the diagnostic and heater reflection heights [*Jones et al.*, 1984], we have measured anomalous absorption on the two diagnostics which were fixed at ±70 kHz from the heater frequency. Two fixed frequency diagnostics were employed to monitor the ambient propagation conditions.

In addition to the generation of small-scale FAI, which are responsible for anomalous absorption, high-power radio waves also produce large-scale changes in the mean electron temperature and electron density [e.g., *Stocker et al.*, 1992]. During the experiments reported here, EISCAT observations of electron temperature and electron density were made at heights between 140 and 600 km, with 22.5-km resolution. The heater-induced changes are obtained as percentages of the ambient values, i.e., $\Delta T_e / T_e$ and $\Delta N_e / N_e$, where $\Delta T_e = T_e - T_{e0}$ and $\Delta N_e = N_e - N_{e0}$, T_e, and T_{e0} and similarly N_e and N_{e0} being the average electron temperature and electron density for any given pump frequency during heater on and heater off periods, respectively. For overdense heating (i.e., the case reported in this paper) the maximum response in $\Delta T_e / T_e$ and $\Delta N_e / N_e$ occurs near the heater reflection height. The values of $\Delta T_e / T_e$ and $\Delta N_e / N_e$ presented below correspond to the altitude (i.e., range gate) closest to the heater reflection height, which for these experiments is approximately 200 km.

Stimulated electromagnetic emission spectra were obtained during the first 3-4 min after the tuning period, while the heater was transmitting CW. For a pump frequency close to the third harmonic of the electron gyrofrequency the spectral features include the continuum, downshifted maximum (DM), downshifted peak (DP), and broad symmetrical structure (BSS). These features have been discussed in great detail by *Stubbe and Kopka* [1990] and *Stubbe et al.* [1994]. The DP and BSS complement each other in the sense that they do not coexist at a given pump frequency. The DP and BSS have only been observed for pump frequencies close to the third harmonic of the electron gyrofrequency, whereas the DM and the continuum have been observed for the other harmonics as well [*Stubbe et al.*, 1984, 1994; *Leyser et al.*, 1989, 1990, 1992]. The DM has been attributed to the presence of heater-induced small-scale irregularities, and therefore this feature is of special interest in studying SEE in conjunction with anomalous absorption.

In order to illustrate the interdependencies among the three different data sets and their characteristic changes with the pump frequency, the measurements obtained from each diagnostic have

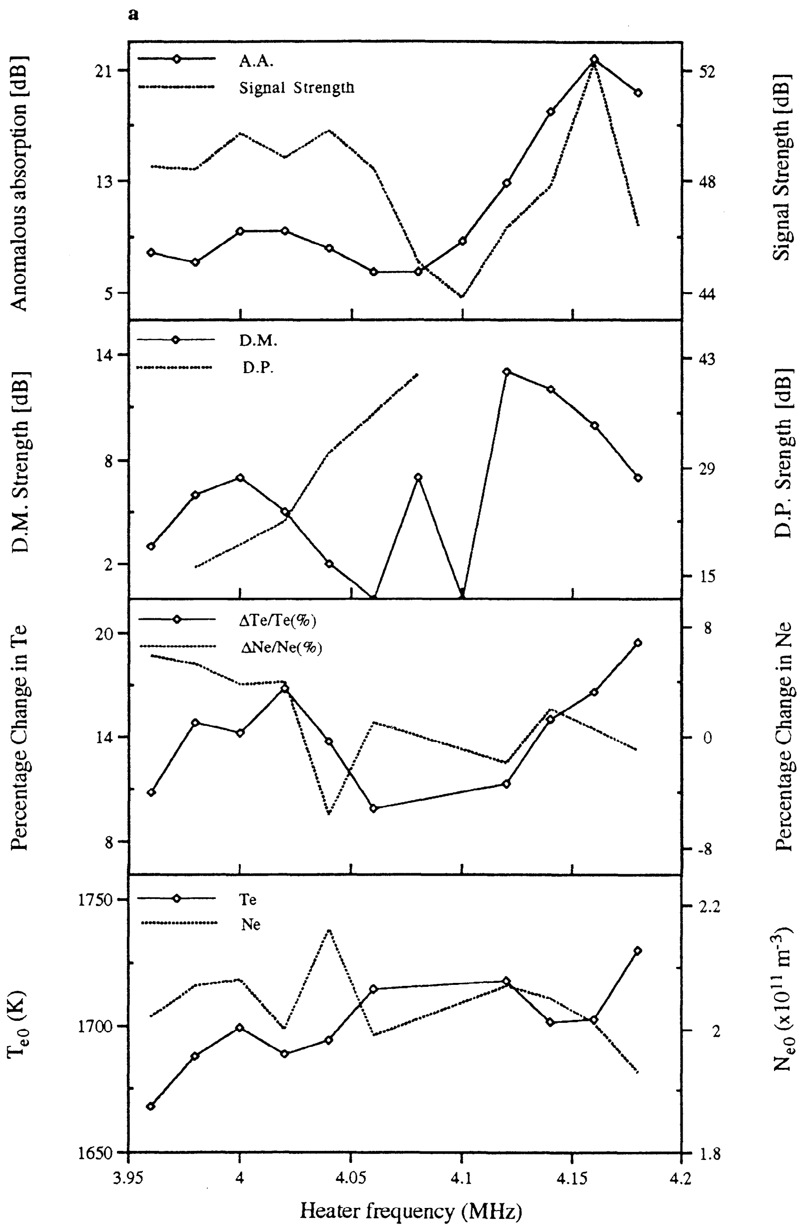

Figure 1. (a) Top panel illustrates anomalous absorption measured on an HF diagnostic wave as a function of pump frequency, together with the relative signal strength of HF diagnostic as a function of time, measured during periods of no heating. Second panel plots the strength of DP and DM as a function of pump frequency. Third panel presents the heater-induced enhancements in electron temperature and density as a function of pump frequency. Fourth panel depicts the ambient values of electron temperature and density measured by EISCAT. Typical errors associated with electron temperature are of the order of 3%, with electron density are 5-10%, while the errors associated with the signal strength are in the range of 0.5-1 dB. The results presented in this figure correspond to the experiment performed on October 5, 1992. The injected frequency was varied in steps of 20 kHz, starting with 3.96 MHz and finishing at 4.18 MHz. (b). The same as Figure 1a except the pump frequency started at 4.18 MHz and was stepped downward in frequency.

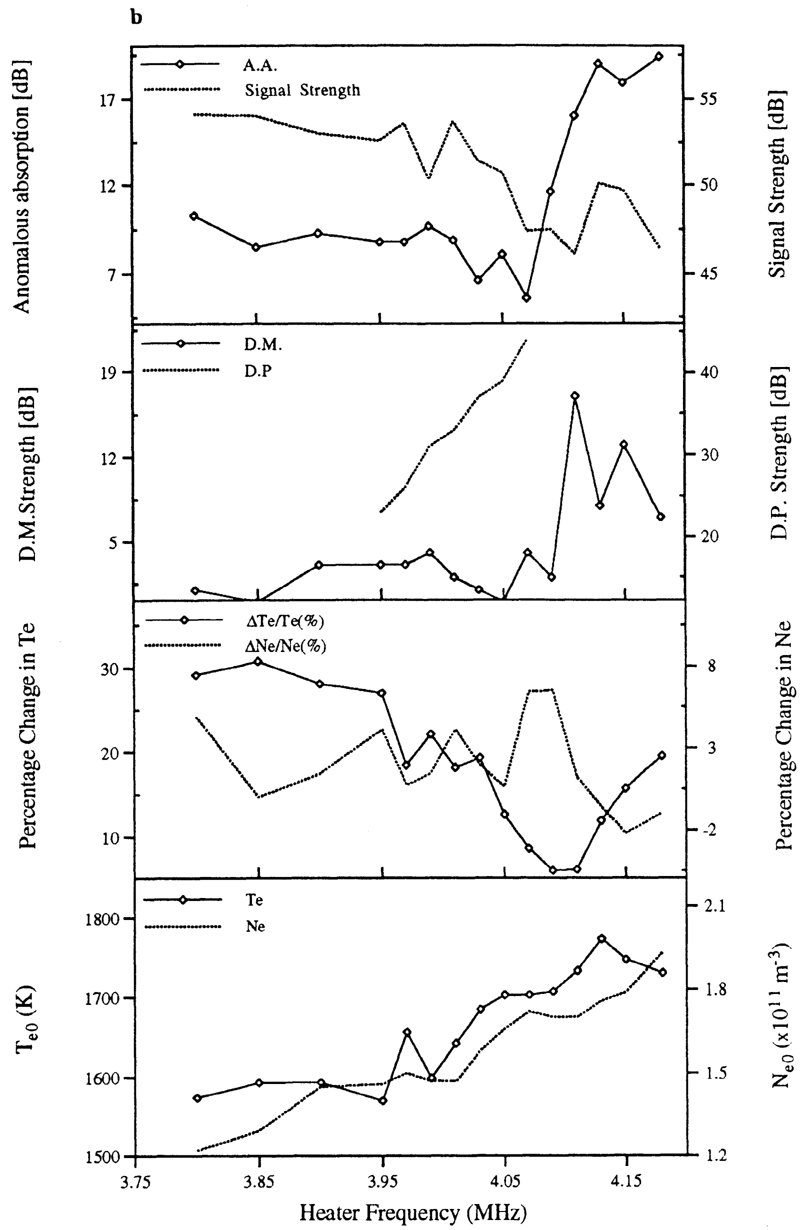

Figure 1. (continued)

been plotted as a function of heater frequency (Figures 1, 2, and 3). In the first panel of each figure the received signal strength of one of the fixed low-power HF diagnostics (i.e., the diagnostic with a fixed frequency of ~500 kHz below the heater frequency) measured during the heater off periods and the anomalous absorption are presented, the second panel illustrates the intensity of the two key features from the SEE spectra (namely, DP and DM), the third panel depicts the percentage changes in T_e and N_e observed by EISCAT near the heater reflection height, and the fourth panel represents the average unheated values of T_e and N_e which indicate the background ionospheric conditions. It should be noted that the EISCAT data were obtained from long-pulse (350 μs) spectra which provide measurements with 22.5-km altitude resolution. Only data from the gate centered at 200 km are presented, since this is the gate closest to the heater reflection height.

The data in Figures 1a and 1b correspond to two consecutive runs of frequency stepping upward and downward, respectively, for an experiment performed on October 5, 1992. From these figures it is clear that the anomalous absorption has a broad minimum centered on f_0 = 4.08 MHz for the first run (Figure 1a), and at f_0 = 4.07 MHz for the second run (Figure 1b) and that it is also asymmetric in frequency with low values of anomalous absorption below the minimum and higher values above. The frequency at which the minimum of anomalous absorption occurs for each run will be referred to as $f_{\min}$ throughout this paper.

The signal strength of the HF probe waves for all four diagnostics (i.e., the two fixed frequency diagnostics and the two diagnostics with constant offset frequency from the heater) have been obtained by averaging the amplitude of the received signal for periods when the heater is turned off, excluding the first 10 s immediately after the heater switch-off in order to allow the signal to recover from anomalous absorption. The signal strength presented in Figures 1-3 is for an O mode probe wave with a fixed frequency of 3.5 MHz for the experiments on October 5 and 6 and 3.8 MHz for the experiment performed on October 8 1992.

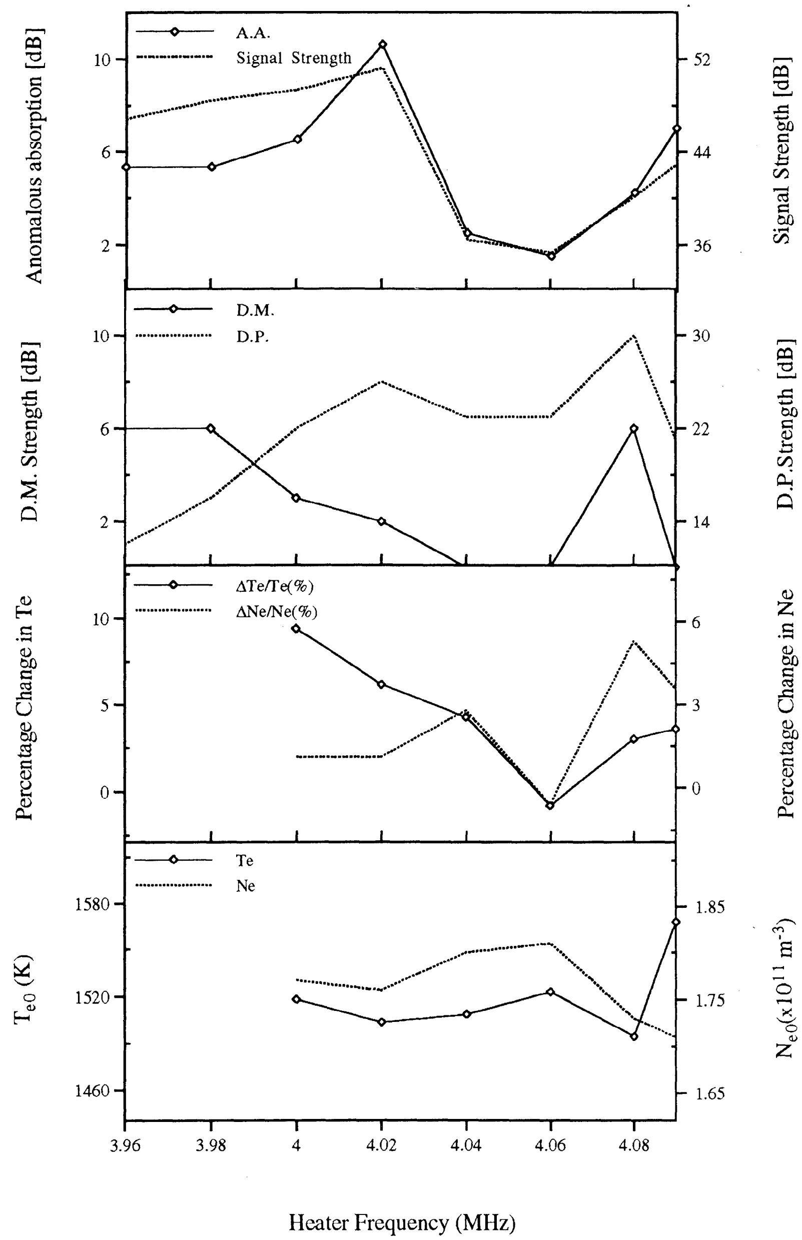

Figure 2. The same as Figure 1a but for the experiment of October 6, 1992. For the first two heater frequencies, EISCAT measurements of electron temperature and density have not been obtained.

Data from both the off-time after the CW part of the heater cycle and after the pulse are included in the average. It is therefore anticipated that the value of the signal strength would fluctuate about a constant level if the ionospheric background condition is unchanged. However, an unexpected minimum in the received signal strength is observed at f_0 = 4.10 MHz for the first run (Figure 1a), and at f_0 = 4.09 MHz for the second run (Figure 1b). In both cases the minimum in signal strength occurred at f_{min} + 20 kHz. The intensity of DM can be presented in two ways [*Stubbe et al.*, 1994]: Either the DM strength represents the measurement from the base line (which is approximately the noise level), or the measurement can represent the discreteness of the downshifted maximum. In the latter case the strength of DM is measured in relation to the level of the right-sided continuum. The strength of DM, presented in panel 2 of Figures 1, 2, and 3 is measured in relation to the right-sided continuum.

The strength of DP in these figures corresponds to the amplitude of this peak above the baseline. In both Figures 1a and 1b the DP appears at a heater frequency approximately 100 kHz below f_{min} and ceases to exist for heater frequencies greater than f_{min}. The strength of this feature increases approximately linearly with increasing heater frequency, and its maximum value occurs at f_{min}. The strength of the DM feature, on the other hand, decreases considerably at f_{min}; i.e., it is no longer a discrete spectral line and becomes part of the continuum.

EISCAT observations of heater-induced changes in T_e and N_e indicate that large-scale heating occurs with elevated electron temperatures as high as 30% of the ambient values (see Figures 1a and 1b for first and second run, respectively). However, the amount of heating varies with changing heater frequency, and a broad minimum where $\Delta T_e / T_e$ is less than 10% in value is observed at f_{min} for the first run and f_{min} +20 kHz for the second

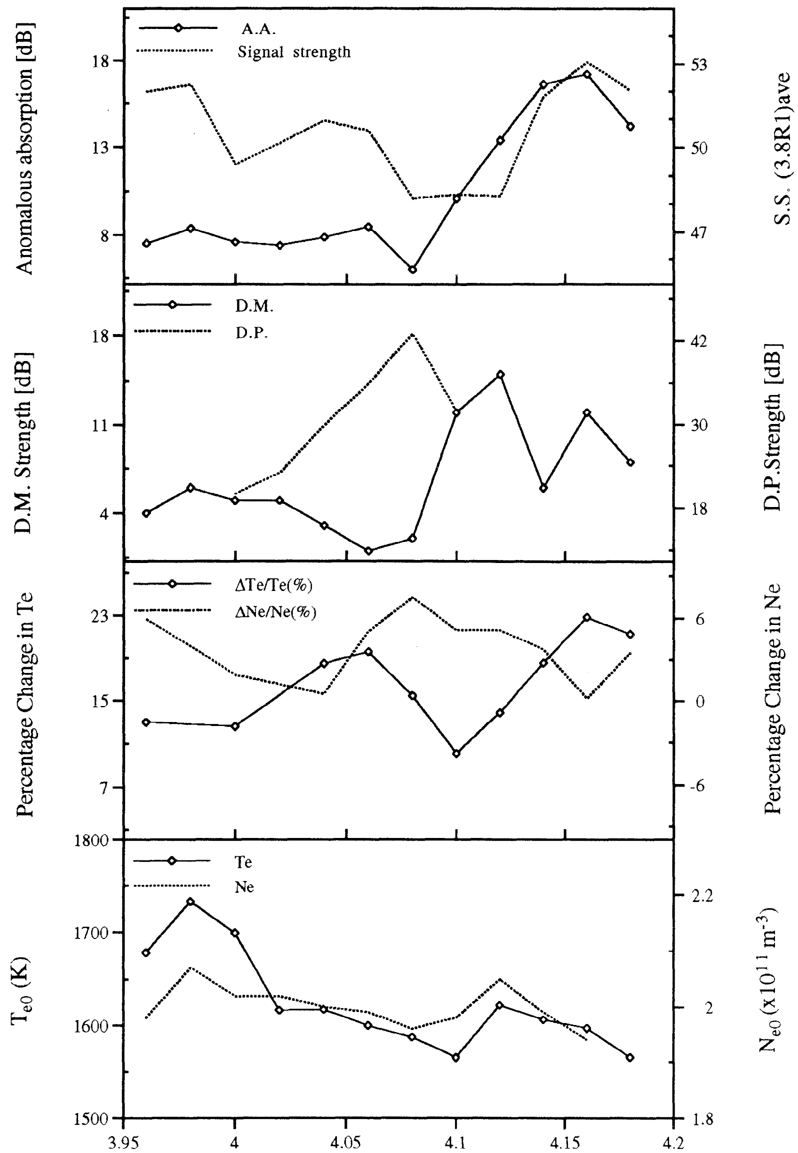

Figure 3. The same as Figure 1a but for the experiment of October 8, 1992.

run. The corresponding changes in N_e are much smaller (less than 7%) and are similar in size to the experimental errors. The ambient values of electron temperature and electron density remain relatively constant during the first run, but a downward trend in N_e can be seen for the second run, when the heater frequency was stepped downward. This decrease in electron density, at the fixed height of 200 km, with time is expected, since sunset occurred shortly after the end of the experiment. The increase in the diagnostic signal strength during the second run is probably a consequence of a reduction in D region absorption.

In Figure 2, observations from the experiment of October 6, 1992, are presented. There is a remarkable correlation between the anomalous absorption and the signal strength at 3.5 MHz for this experiment. Both anomalous absorption and signal strength exhibit a broad minimum centered at f_0 = 4.06 MHz. The DM and the heater-induced changes in the electron temperature and density also have minimum values at this frequency. There are no EISCAT data available for the first two heater frequencies.

Data pertaining to the experiment performed on October 8, 1992, are illustrated in Figure 3. The minimum of anomalous absorption occurs at f_0 = 4.08 MHz, whereas the signal strength of the fixed frequency diagnostic (3.8 MHz) exhibits a minimum at f_0 = 4.10 MHz. The minimum in the DM feature also coincides with that of the anomalous absorption. EISCAT observations of large-scale heating indicate minimum changes in electron temperature of less than 10% at f_0 = 4.10 MHz and maximum changes of up to 23% for frequencies greater than 4.15 MHz. Corresponding changes in electron density of less than 8% are observed. The background values of T_e and N_e remain reasonably constant for all heater frequencies.

Considering the results reported here, the main findings are outlined as follows:

1. Anomalous absorption of HF diagnostic wave exhibits a broad minimum at heater frequencies close to the third harmonic of the electron gyrofrequency.

2. Anomalous absorption of HF diagnostic wave is asymmetric

with respect to its minimum, with high values of anomalous absorption (~20 dB) above and low values (<10 dB) below the minimum.

3. The strength of DM correlates well with the measured anomalous absorption of the HF diagnostic wave and has a broad minimum at the heater frequency for which the minimum of anomalous absorption occurs.

4. The strength of DP increases linearly with increasing heater frequency and has a maximum value at heater frequency for which the minimum of anomalous absorption occurs. This feature ceases to exist for heater frequencies just above the third electron gyroharmonic; instead the SEE spectra exhibits a BSS.

5. A minimum is also observed in the signal strength of a HF diagnostic wave measured while the heater was off (A_{off}). The time when this minimum occurs coincides with the heater off period after the heater was operating at a frequency close to f_{min} (i.e., the frequency at which the minimum in anomalous absorption is observed). The minimum in diagnostic signal strength has been observed systematically for all runs of the experiments, including the run where the heater was stepped down in frequency, and for all four diagnostics (i.e., the two fixed frequency diagnostics and the two diagnostics with constant offset frequency from the heater). It should be noted that during previous heating experiments, for which the heater frequency was fixed throughout the experiment, A_{off} was approximately constant [see *Robinson*, 1989].

6. A reduction in the ambient F region electron density occurs simultaneously with an increase in A_{off} (see Figure 1b).

7. The heater-induced electron temperature enhancement, which varies with changing the pump frequency, is at a minimum when A_{off} is also at a minimum.

These points are addressed in the next section.

4. Discussions

The results reported in section 3 reveal the sensitivity of experimental observations to the pump frequency. Measurements obtained from all three diagnostics employed during these experiments suggests that different mechanisms are involved when the pump frequency is in the vicinity of the third harmonic of the electron gyrofrequency. Therefore it is useful to discuss the results after dividing them into two categories, "universal" (i.e., those features that exist for all pump frequencies) and "gyro" (the features that only exist when the pump frequency is close to the harmonics of the electron gyrofrequency), as was first suggested by *Stubbe et al.* [1994] for explaining the SEE features. According to these authors, the so-called universal features are physically connected with each other via striations excited by the pump at the upper hybrid resonance region. It is generally believed that the small-scale FAI (striations) are formed by UH waves, which can be excited through a thermal oscillating two stream instability (TOTSI) [*Grach et al.*, 1977, 1981; *Das and Fejer*, 1979; *Dysthe et al.*, 1983; *Lee and Kuo*, 1983]. The importance of UH waves for the formation of striations has also been realized through the trapping of these waves in density depletions [*Vas'kov and Gurevich*, 1975, 1984; *Dysthe et al.*, 1982]. The ohmic heating from the trapped UH waves in density cavities provides the necessary positive feedback for the growth of striations. On the other hand, the anomalous or wideband absorption of low-power probe HF radio waves propagating through the heated region is due to the presence of striations in the vicinity of the UH resonance region [*Vas'kov and Gurevich*, 1975, 1977; *Graham and Fejer*, 1976; *Das and Fejer*, 1979; *Stubbe and Kopka*, 1980; *Kuo and Lee*, 1982; *Stubbe et al.*, 1982a, b; *Dysthe et al.*, 1983; *Jones et al.*, 1984, 1986; *Robinson*, 1988, 1989]. Further, the UH waves have been considered [*Leyser*, 1991] to be the pump for the parametric excitation of the DM feature seen in the SEE spectra. *Leyser et al.* [1994] have argued that because of the linear dispersion characteristics of UH waves, these waves cannot exist in a narrow bandwidth around the harmonics of the electron gyrofrequency.

Mjølhus [1993] found that as the pump frequency approaches the harmonics of the electron gyrofrequency, the trapping of UH waves decreases, and hence the growth of the striations is suppressed. Clearly, a weakening of the striations leads to a corresponding reduction of the anomalous absorption and suppression of the DM feature.

Many theories [see *Mjølhus*, 1993; *Rao and Kaup,* 1992; *Bud'ko and Vas'kov*,1992; *Goodman et al.*, 1993; *Tripathi and Liu*, 1993; *Huang and Kuo*, 1994; *Huang et al.*, 1995] discuss the importance of electron Bernstein (EB) waves when the pump frequency is near a gyroharmonic. EB waves are high-frequency electrostatic waves propagating orthogonally to the magnetic field and are believed to play an important role in the generation of SEE.

Huang and Kuo [1994] have considered the parametric excitation of EB and UH waves by the O mode HF pump wave via the thermal oscillating two-stream instability. Their calculation indicates that the dispersion relations of EB waves and UH waves become coupled in the frequency range around the electron cyclotron harmonic frequency. The effect of this coupling, for the case of the heater frequency operating near the third gyroharmonic, is that the instability zone of upper hybrid waves below the upper hybrid resonance layer becomes very small, and thus the source wave of the DM feature is effectively suppressed. In addition, these authors have demonstrated that the parametric excitation of EB waves is relatively weak compared to the excitation of UH waves, and it can only exist in a narrow wavelength region, provided the heater frequency is slightly higher than the harmonic of the electron gyrofrequency. *Stubbe and Kopka* [1990] have suggested that the BSS feature could be generated by a two-step process. The first step involves the decay of the EB pump wave into a lower hybrid wave and a secondary EB wave. This process can then be followed by the scattering of the primary EB wave, off the lower hybrid wave, to produce BSS feature. An alternative approach has recently been studied by *Huang et al.* [1995], in which EB waves and FAI are excited parametrically by the HF heater through a thermal oscillating two-stream instability. In the second stage the heater-excited EB wave then parametrically excites frequency upshifted and downshifted EB sidebands, together with a lower hybrid decay mode through a modulational instability. According to these authors, EB sidebands can be scattered off the field-aligned density irregularities to produce the frequency-upshifted and downshifted sidebands manifesting the BSS feature.

SEE features have also been considered to be related to the production of energetic electrons [*Dimant et al.*, 1992]. Generation of suprathermal electrons by high-power radio waves is a well-known phenomenon [*Fejer and Graham*, 1974; *Weinstock*, 1974; *Gurevich et al.*, 1985; *DuBois et al.*, 1990], and direct observation of electron fluxes with energies in excess of 20 eV have been reported by *Carlson et al.* [1982]. *Carlson et al.*'s observations, which were made at nighttime (i.e., in the absence of photoelectrons), indicated the presence of energetic electrons throughout their observing region, which extended from the heater reflection height to some 30 km below that height. They also observed that the flux of downgoing suprathermal electrons was 2 to 3 times that of the upgoing energetic electrons. *Fejer and Sulzer* [1987] have reported both daytime and nighttime observations of enhanced plasma line due to suprathermal electrons. According to their observations, in the presence of photoelectrons the observed plasma line enhancement was about 2 orders of magnitude greater than the nighttime enhancement. They have attributed the nighttime effect to multiple acceleration of electrons from the high-energy tail of the Maxwellian distribution, and the daytime effect to a modification in the distribution function of photoelectrons. The production of such energetic electrons can lead to airglow emission and artificial ionization. According to the theoretical work of *Vas'kov and Ivanov-Kholodiny* [1991], only a small fraction of the energy of the high-power radio wave (~10%) is expended in generating such high energetic particles. These authors have demonstrated that for heater frequencies close to harmonics of the electron gyrofrequency the distribution function of the accelerated electrons may have a long tail with energies of the order of 1 keV. *Dimant et al.* [1992] have studied the effect of intense plasma turbulence generated by HF waves on an electron distribution function. Their calculations indicate that for pump frequencies close to the electron gyroharmonics the whole turbulence region is localized within a thin altitude layer situated at the upper hybrid resonance region. This results in the formation of a high-energy tail in the electron distribution.

Although the production of fast electrons occurs in a thin layer in the *F* region below the reflection height of the pump wave, provided that these highly energetic electrons have acquired energies of the order of keV, they can reach to much lower heights before they lose their energies. Electrons with energies in the range of 1-10 keV can produce ionization in the height region of 150-100 km, respectively [see *Hargreaves*, 1992, Table 6.1 and Figure 6.6]. Hence it is more likely that the ionized patches produced by energetic electrons are in the lower altitudes where the concentration of neutral particles is high. The geometry of our experiment, including the refraction of the heater beam and the location of the probe transmitters and receivers, ensures that the probe wave could propagate through the *D* and *E* regions affected by the flux of the energetic electrons. The time constant associated with this ionization depends on the recombination process, which itself is a function of electron density and temperature. The relaxation time (τ_n) for electron concentration varies considerably with altitude as well as with changes in the ambient ionosphere. Typical daytime and nighttime values for τ_n, at a height of 100 km, are 52 and 2000 s, respectively [see *Gurevich*, 1978, Table 13]. In order to investigate the time constant for the process responsible for the observed minimum in the diagnostic signal strength the following procedures have been undertaken for obtaining the signal strength of the HF probe waves as a function of time. (1) The first 10 s of the data immediately after the heater switch-off have been excluded in

Signal Strength during heater off, 5 Oct. 92 (1st. run)

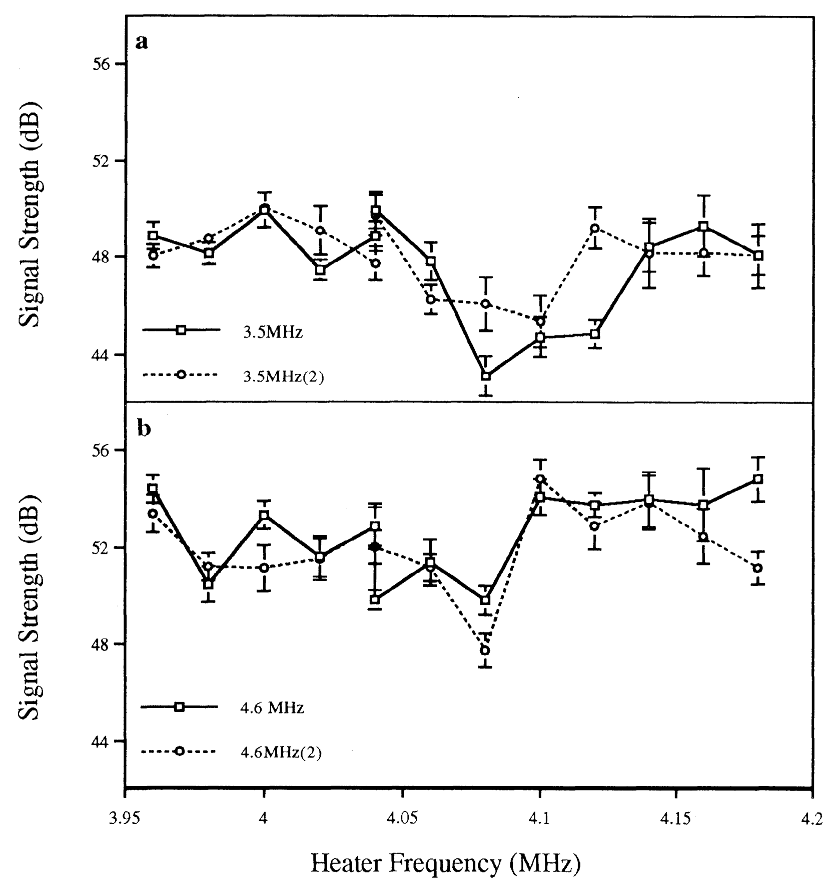

Figure 4. (a). Amplitude of the low-power HF probe waves having a fixed frequency of 3.5 MHz averaged for the two periods of 10-35 s (solid line) and 35-60 s (dashed line) after heater is switched off as a function of heater frequency for the first run of the experiment of October 5 1992. (b) The same as Figure 4a but for the fixed frequency diagnostic operating at 4.6 MHz.

order to allow the signal to recover from anomalous absorption. (2) The amplitudes of the received signal have been averaged for periods of 10-35 s and 35-60 s after the heater is turned off for all four diagnostics (i.e., the two fixed frequency diagnostics and the two diagnostics with constant offset frequency from the heater). The data from both off periods in the heater cycle have been included in the averaging process. The results for the two fixed frequency diagnostics are presented in Figures 4, 5, 6, and 7. These figures correspond to the experiments of October 5 (first and second run), 6, and 8, 1992, respectively. The solid line in each figure presents the first average (i.e., the average obtained for the period of 10 to 35 s after the heater is switched off), and the dashed line corresponds to the second average obtained for the period of 35-60 s after the heater is switched off. From these figures it can be seen that the minimum in the diagnostic signal strength persists during the whole period of heater off. This finding indicates that the process responsible for the reduced signal strength must have a time constant of the order of the heater cycle (1 min) or more. Therefore increased absorption and scattering due to the ionized patches produced by energetic electrons may provide an explanation of the observed reduction in the signal strength.

Large-scale heating of the F region plasma at high latitudes is believed to be due mostly to the anomalous absorption of the pump wave [e.g., *Robinson*, 1989]. Therefore the height-integrated heating rate Q can be approximated as:

$$Q \propto |E|^2\left(1-e^{-\Gamma_F}\right) \qquad (2)$$

where $E = E_0 e^{-\left(\Gamma_D/4\right)}$, $|E|^2$ is the transmitted power, and Γ_D and Γ_F are the absorption coefficients of HF waves due to D and F region absorption. F region absorption includes the contribution from both anomalous and collisional absorption (i.e., $\Gamma_F = \Gamma_a + \Gamma_c$ where Γ_a and Γ_c are the anomalous and collisional absorption coefficients, respectively). Figure 8a illustrates the correlation between the electron temperature enhancement observed by EISCAT and the measured anomalous absorption (Γ_a) for all the experiments reported in this paper. In Figure 8b the correlation, for the same set of experiments, is made between the enhancement in electron temperature and the received diagnostic signal strength for periods of no heating which provides a measure of D region absorption. Clearly, high values of diagnostic signal strength correspond to low values of Γ_D and consequently increased heating rate. Although there seems to be a reasonable correlation between the T_e enhancement and received diagnostic signal strength, the correlation between T_e and anomalous absorption is very poor. This is understandable, since for large values of anomalous absorption, provided $\Gamma_F \approx \Gamma_a$, equation (2) indicates that the second term in parentheses is negligible. Therefore if the heating of the F region plasma is caused by anomalous absorption process, then the correlation coefficient between the T_e enhancement and anomalous

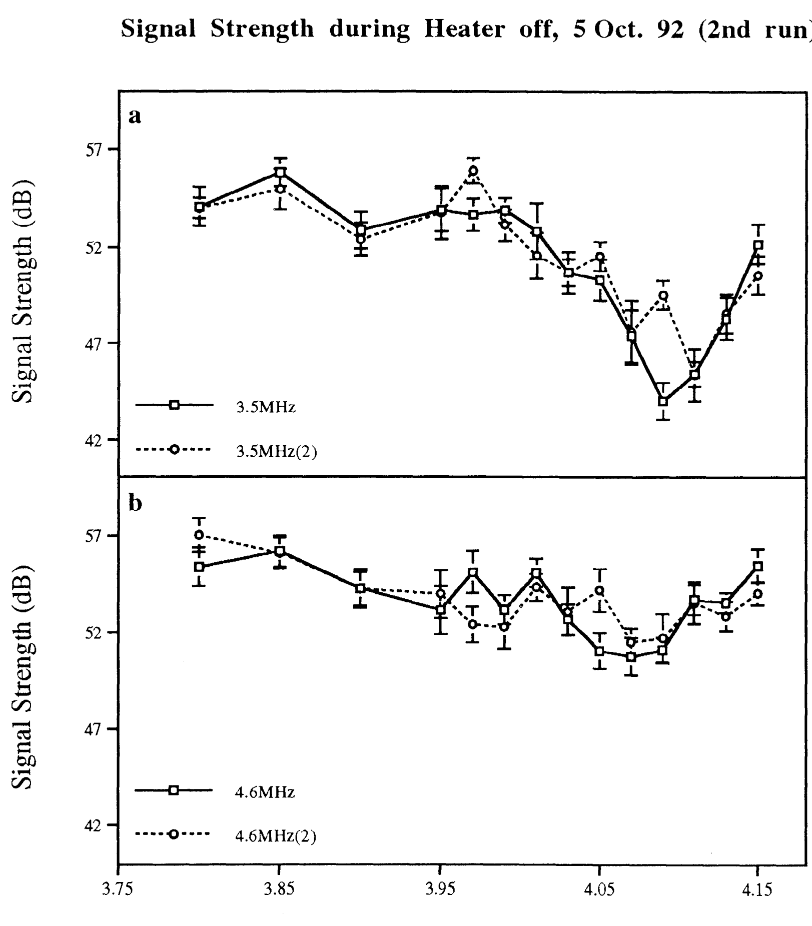

Figure 5. The same as Figure 4 but for the second run (i.e., frequency stepping downward) of the experiment performed on October 5 1992.

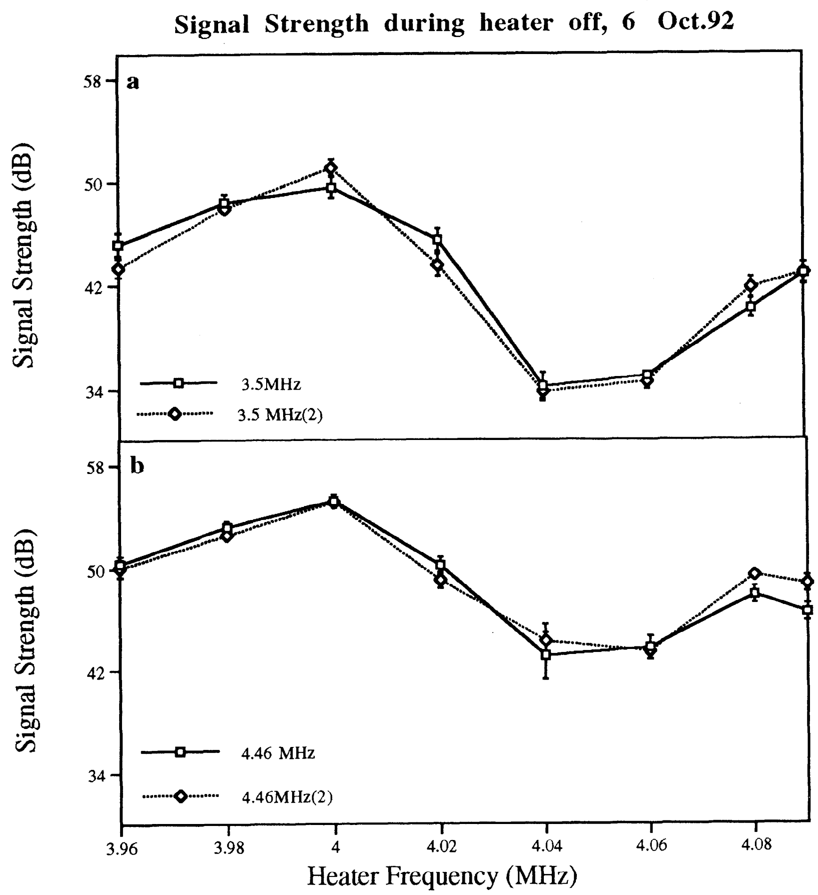

Figure 6. The same as Figure 4 but for the experiment of October 6 1992.

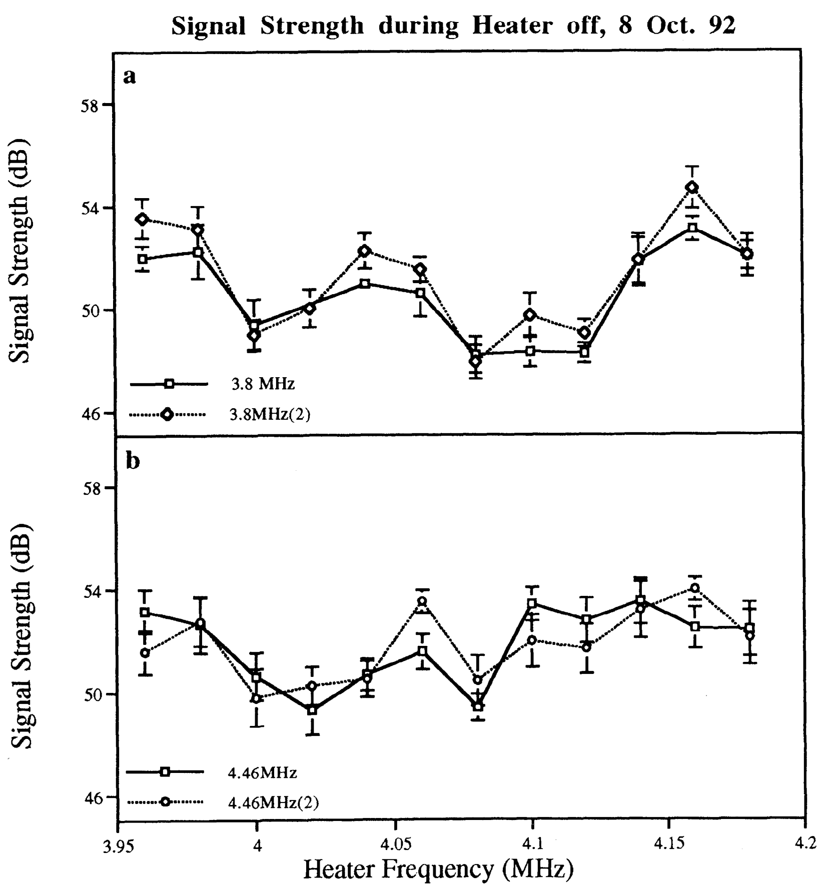

Figure 7. The same as Figure 4 but for the experiment of October 8 1992. The two fixed frequency diagnostics for this experiment were operating at (a) 3.8 and (b) 4.46 MHz.

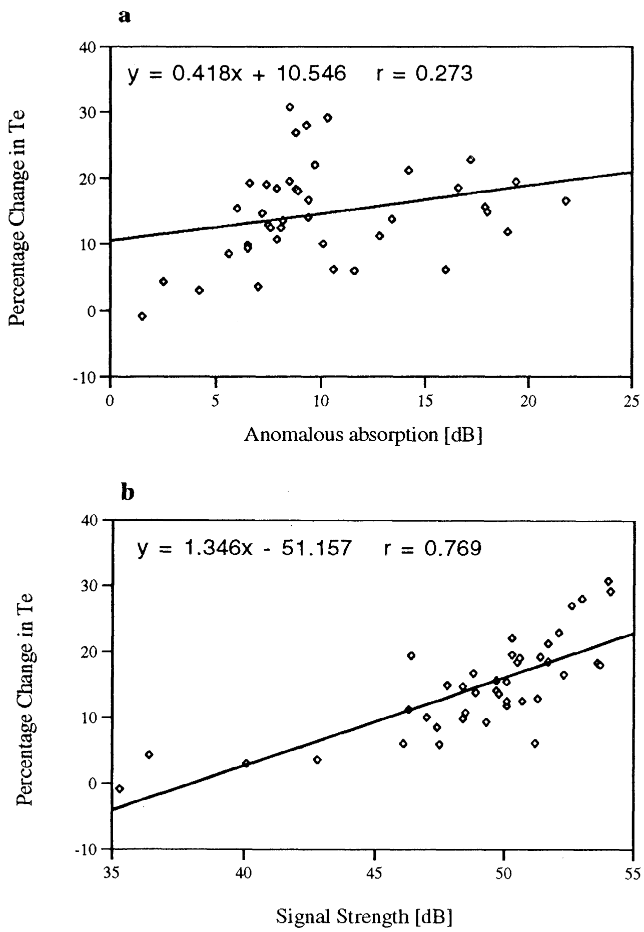

Figure 8. (a) Heater-induced electron temperature enhancement plotted against the anomalous absorption of HF diagnostic wave measured at the same heater frequency for all the data obtained from the three experiments performed on October 5, 6, and 8, 1992. (b) The same as Figure 8a but the enhancement in electron temperature is plotted as a function of the amplitude of the low-power HF diagnostic wave having a fixed frequency of 3.5 MHz. The data representing the signal strength is the averaged signal amplitude over the periods of "heater off," excluding the first 10 s after the heater is switched off, in order to represent the ambient ionospheric condition. The solid line in each panel is a linear regression fit to the data.

absorption will be significant only for low values of Γ_a. This point has been clarified by plotting the T_e enhancement as a function of anomalous absorption and signal strength for the two regimes, i.e., close to the third gyroharmonic (Figure 9), where the anomalous absorption is low, and away from the third harmonic (Figure 10). Comparison of the correlation coefficients for the two cases leads us to the conclusion that the heating in the F region is in fact due to anomalous absorption. Also, Figures 8, 9, and 10 emphasize the importance of ionospheric conditions (i.e., D and E region absorption of HF pump wave) in heating experiments.

5. Conclusions

The observations reported in this paper are to date the most comprehensive, with regard to HF heating at a pump frequency close to the third electron gyroharmonic. The interdependencies among the simultaneous measurements made by the three diagnostics employed (i.e., T_e and N_e from EISCAT data, anomalous absorption and the signal strength obtained from the low-power HF transmitter and receiver system, and the SEE features observed by spectrum analyzer) have provided some new findings as well as confirmation of some of the previously reported results. The new results include the unexpected minimum in the level of signal strength for the period of no heating immediately after the pump has operated at the third gyroharmonic and the reduced heating of the electron gas when the pump frequency is close to the third gyroharmonic, while the F region observation of electron density has shown very little change with the variation of the heater frequency. The reduction in anomalous absorption, the quenching of DM feature close to harmonics of the electron gyrofrequency, and the disappearance of DP and appearance of BSS for pump frequencies above the third electron gyroharmonic confirm the results of previous publications [see *Stubbe and Kopka*, 1990; *Stocker et al.*, 1993; *Stubbe et al.*, 1994].

Although the processes involved when heater frequency is well away from the third electron gyroharmonic have been explained in the literature, the process responsible for the asymmetry in the observed anomalous absorption has yet to be identified. The complexity of results obtained during ionospheric modification with the pump frequency close to the third electron gyroharmonic has made it difficult to identify all the possible processes involved. Recently developed theories [*Mjølhus*, 1993; *Huang and Kuo*, 1994; *Leyser et al.*, 1994] can explain the suppression of UH waves close to the third electron

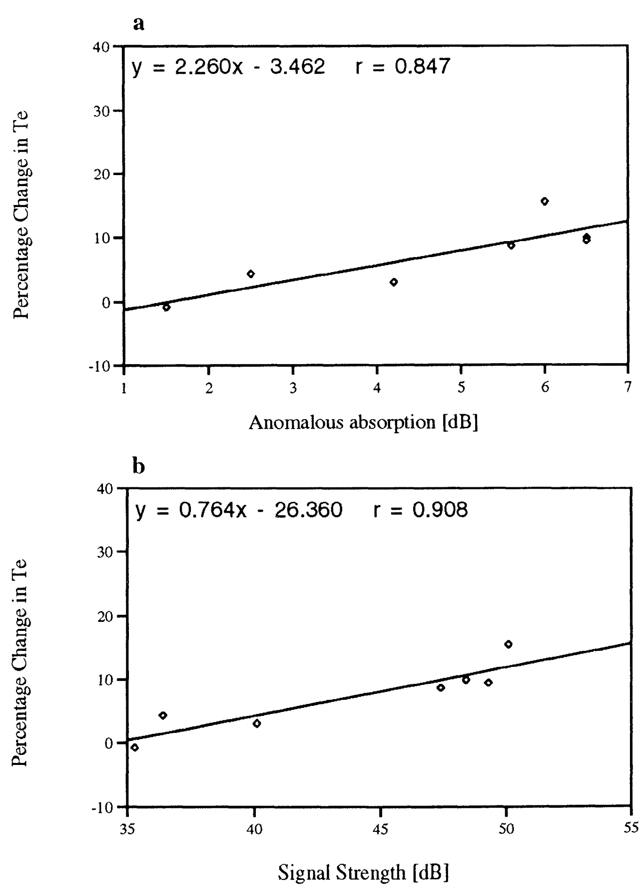

Figure 9. The same as Figure 8 but only the data corresponding to heater frequencies in the vicinity of the third harmonic of the electron gyrofrequency (i.e., the frequencies for which the minimum in anomalous absorption occurs) have been included.

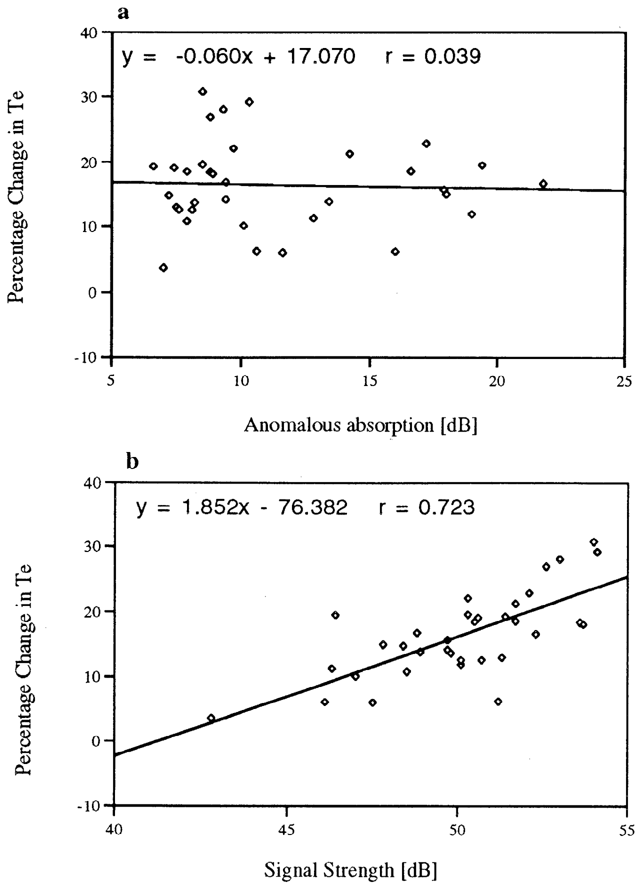

Figure 10. The same as Figure 8 but excluding the data corresponding to heater frequencies for which the minimum of anomalous absorption has been observed.

gyroharmonic; this in turn leads to the weakening of FAIs and can therefore explain the quenching of the DM feature and the minimum in anomalous absorption. With regard to our experimental results the *F* region heating is governed by anomalous absorption of HF pump wave, and therefore the reduced heating at frequencies close to the third electron gyroharmonic, where anomalous absorption is minimum, is understandable. There are also several attempts in the literature to explain the generation of BSS feature [*Stubbe and Kopka*, 1990; *Huang et al.*, 1995] and DP feature [*Stubbe et al.*, 1984; *Leyser and Thidé*, 1988]. Observations reported in this paper as well as previous experimental observations of SEE features [e.g., *Stubbe et al.*, 1994] indicate that both DP and BSS features are "gyrofeatures" and complementary to each other. Hence it is expected that these features will be treated in a unified theory. As yet such a theory has not been reported.

Although it has been theoretically demonstrated that for heater frequencies close to the harmonics of the electron gyrofrequency the production of highly energetic electrons with energies in the keV range is viable [*Villalon*, 1989; *Vas'kov and Ivanov-Kholodiny*, 1991], these predictions are at least 1 order of magnitude higher than the observed values reported [*Carlson et al.*, 1982; *Fejer and Sulzer* ,1987]. One can argue that previous observations were made at arbitrary heater frequencies, whereas the mechanism for the generation of high-energy electrons (in the keV range) is favorable when the heater frequency is chosen to be at the harmonics of the electron gyrofrequency. Provided that our observation of reduced signal strength (for periods of no heating immediately after the heater operated at the third harmonic of the electron gyrofrequency) is related to the ionization patches produced by the energetic electrons, further experimental observations are required in order to find out the exact altitude and the efficiency of the production of artificial ionization by energetic electrons during heating at the third harmonic of the electron gyrofrequency. Also, the relationship between the SEE features and high-energy electrons needs to be investigated.

Acknowledgments. We wish to thank A. V. Gurevich for his useful suggestions in interpreting the data contained in this paper. We would also like to thank H. Gegner for operating the heater. Two of us (F.H. and A.J.S.) were supported by SERC grants GRF80784 and GRH32025 during the course of this work.

The Editor thanks Thomas B. Leyser and Einar Mjølhus for their assistance in evaluating this paper.

References

Belyakova, V. N., et al., The features of excitation of plasma turbulence by a high power radio wave field under even-order gyro resonance conditions, *Geomagn. Aeron., 31*, 367-370, 1991.

Bud'ko, N. I., and V. V. Vas'kov, Four-wave decay of a powerful radio wave under multiple electronic gyro resonance conditions, *Geomagn. Aeron., 32*, 63-70, 1992.

Carlson, H. C., V. B. Wickwar, and G. P. Mantas, Observations of fluxes of suprathermal electrons accelerated by HF excited instabilities, *J. Atmos. Terr. Phys., 44*, 1089-1100, 1982.

Das, A. C. , and J. A. Fejer, Resonance instability of small-scale field-aligned irregularities, *J. Geophys. Res., 84*, 6701-6704, 1979.

Dimant, Y. S., A. V. Gurevich, and K. P. Zybin, Acceleration of electrons in the ionosphere under the action of intense radio waves near electron cyclotron harmonics, *J. Atmos. Terr. Phys., 54*, 425-436, 1992.

DuBois, D. F., H. A. Rose, and D. Russell, Excitation of strong Langmuir turbulence in plasmas near critical density: Application to HF heating of the ionosphere, *J. Geophys. Res., 95*, 21,221-21,272, 1990.

Dysthe, K. B., E. Mjølhus, H. L. Pesceli, and K. Rypdal, Thermal cavitons, *Phys. Scr., T2 (2)*, 548-559, 1982.

Dysthe, K. B., E. Mjølhus, H. L. Pesceli, and K. Rypdal, A thermal oscillating two-stream instability, *Phys. Fluids, 26*, 146-157, 1983.

Fejer, J. A., and K. N. Graham, Electron acceleration by parametrically excited Langmuir waves, *Radio Sci., 9*, 1081-1084, 1974.

Fejer, J. A., and M. P. Sulzer, Observation of suprathermal electron fluxes during ionospheric modification experiments, *J. Geophys. Res., 92*, 3441-3444, 1987.

Fejer, J. A., C. A. Gonzales, H. M. Ierkic, M. P. Sulzer, C. A. Tepley, L. M. Duncan, F. T. Djuth, S. Ganguly, and W. E. Gordon, Ionospheric modification experiments with the Arecibo heating facility, *J. Atmos. Terr. Phys., 47*, 1165-1179, 1985.

Goodman, S., B. Thidé, and L. Erukhimov, A combined parametric and conversion mechanism for upshifted stimulated electromagnetic emissions, *Geophys. Res. Lett., 20*, 735-738, 1993.

Grach, S. M., A. N. Karashtin, N. A. Mityakov, V. O. Rapoport, and V. Y. Trakhtengertz, Parametric interaction between electromagnetic radiation and the ionospheric plasma, *Radio Phys. Quantum Electron.*, Engl. Transl., *20*, 1254-1258, 1977.

Grach, S. M., N. A. Mityakov, V. O. Rapoport, and V. Y. Trakhtengertz, Thermal parametric turbulence in a plasma, *Physica, 2D*, 102-106, 1981.

Graham, K.N., and J. A. Fejer, Anomalous radio wave absorption due to heating effects, *Radio Sci., 11*, 1057-1063, 1976.

Gurevich, A.V., *Nonlinear Phenomena in the Ionosphere*, Springer-Verlag, New York, 1978.

Gurevich, A. V., Y. S. Dimant, G. M. Milikh, and V. V. Vas'kov, Multiple acceleration of electrons in the regions of high-power radio-wave reflection in the ionosphere, *J. Atmos. Terr. Phys., 47*, 1057-1070, 1985.

Hargreaves, J. K., *The Solar-Terrestrial Environment,* Cambridge Univ. Press, New York, 1992.

Huang, J., and S. P. Kuo, Oscillating two-stream instability in the high latitude ionosphere, *J. Geophys. Res., 99* (A2), 2173-2181, 1994.

Huang J., S. P. Kuo, and H. L. Zhou, A theoretical study on the broad symmetric structure in the stimulated electromagnetic emission spectrum, *J. Geophys. Res., 100,* 1639-1645, 1995.

Jones, T. B., T. Robinson, P. Stubbe, and H. Kopka, Frequency dependence of anomalous absorption caused by high power radio waves, *J. Atmos. Terr. Phys., 46,* 1027-1035, 1984.

Jones, T. B., T. R. Robinson, P. Stubbe, and H. Kopka, EISCAT observations of the heated ionosphere, *J. Atmos. Terr. Phys., 48,* 1027-1035, 1986.

Kuo, S. P., and M. C. Lee, On parametric excitation of plasma modes at upper-hybrid resonance, *Phys. Lett. A, 91,* 444-446, 1982.

Lee, M. C., and S. P. Kuo, Excitation of upper-hybrid waves by a thermal parametric instability, *Plasma Phys., 30,* 463-478, 1983.

Leyser, T. B., Parametric interaction between upper hybrid and lower hybrid waves in heating experiments, *Geophys. Res. Lett., 18,* 408-411, 1991.

Leyser, T. B., and B. Thidé, Effect of pump-induced density depletions on the spectrum of stimulated electromagnetic emissions, *J. Geophys. Res., 93,* 8681-8688, 1988.

Leyser, T. B., B. Thidé, H. Derblom, Å. Hedberg, B. Lundborg, P. Stubbe, and H. Kopka, Stimulated electromagnetic emission near electron cyclotron harmonics in the ionosphere, *Phys. Rev. Lett., 63,* 1145-1147, 1989.

Leyser, T. B., B. Thidé, H. Derblom, Å. Hedberg, B. Lundborg, P. Stubbe, and H. Kopka, Dependence of stimulated electromagnetic emission on the ionosphere and pump wave, *J. Geophys. Res., 95,* 17,233-17,244, 1990.

Leyser, T. B., B. Thidé, S. Goodman, M. Waldenvik, E. Veszelei, S. M. Grach, A. N. Karashtin, G. P. Komrakov, and D. S. Kotik, Narrow cyclotron harmonic absorption resonances of stimulated electromagnetic emission in the ionosphere, *Phys. Rev. Lett., 68,* 3299-3302, 1992.

Leyser, T. B., B. Thidé, M. Waldenvik, and S. Goodman, Spectral structure of stimulated electromagnetic emissions between electron cyclotron harmonics, *J. Geophys. Res., 98,* 17,597-17,606, 1993.

Leyser, T. B., B. Thidé, M. Waldenvik, E. Veszelei, V. L. Frolov, S. M. Grach, and G. P. Komrakov, Downshifted maximum features in stimulated electromagnetic emission spectra, *J. Geophys. Res., 99,* 19,555-19,568, 1994.

Lobachevsky, L. A., Y. V. Gruzdev, V. Y. Kim, G. A. Mikhaylova, V. A. Panchenko, V.P. Polimatidi, V. A. Puchkov, V. V. Vas'kov, P. Stubbe, and H. Kopka, Observations of ionospheric modification by the Tromsø heating facility with the mobile diagnostic equipment of IZMIRAN, *J. Atmos. Terr. Phys., 54,* 75-85, 1992.

Mjølhus, E., On the small scale striation effect in ionospheric radio modification experiments near harmonics of the electron gyro frequency, *J. Atmos. Terr. Phys., 55,* 907-918, 1993.

Rao, N. N., and D. J. Kaup, Excitation of electron cyclotron harmonic waves in ionospheric modification experiments, *J. Geophys. Res., 97,* 6323-6341, 1992.

Rishbeth, H., and A. P. VanEyken, EISCAT: Early history and first ten years of operation, *J. Atmos. Terr. Phys., 55,* 525-542, 1993.

Rishbeth, H., and P. J. S. Williams, The EISCAT ionospheric radar: The system and its early results, *Q. J. R. Astron. Soc., 26,* 478-512, 1985.

Robinson, T. R., The excitation of plasma waves and irregularities in the ionosphere by means of high power radio waves, *Plasma Phys. Controlled Fusion, 30,* 45-56, 1988.

Robinson, T. R., The heating of the high latitude ionosphere by high power radio waves, *Phys. Rep., 179,* 79-209, 1989.

Stocker, A. J., F. Honary, T. R. Robinson, T. B. Jones, P. Stubbe, and H. Kopka, EISCAT observations of large scale electron temperature and electron density perturbations caused by high power HF radio waves, *J. Atmos. Terr. Phys., 54,* 1555-1572, 1992.

Stocker, A. J., F. Honary, T. R. Robinson, T. B. Jones, and P. Stubbe, Anomalous absorption during artificial modification at harmonics of the electron gyrofrequency, *J. Geophys. Res., 98,* 13,627-13,634, 1993.

Stubbe, P., and H. Kopka, Modification of the *F* -region by powerful radio waves, in *Exploration of the Upper Atmosphere,* edited by C. S. Deehr and J. A. Holtet , pp.83-98, D. Reidel, Norwell, Mass., 1980.

Stubbe, P., and H. Kopka, Stimulated electromagnetic emissions in a magnetised plasma: A new symmetric spectral feature, *Phys. Rev. Lett., 65,* 183-186, 1990.

Stubbe, P., H. Kopka, T. B. Jones, and T. Robinson, Wide band attenuation of radio waves caused by powerful HF waves: Saturation and dependence of ionospheric variability, *J. Geophys. Res., 87,* 1551-1555, 1982a.

Stubbe, P., et al., Ionospheric modification experiments in northern Scandinavia, *J. Atmos. Terr. Phys., 44,* 1025-1041, 1982b.

Stubbe, P., A. J. Stocker, F. Honary, T. R. Robinson, and T. B. Jones, Stimulated electromagnetic emissions and anomalous HF wave absorption near electron gyroharmonics, *J. Geophys. Res., 99,* 6233-6246, 1994.

Stubbee, P., A. J. Stocker, F. Honary, T. R. Robinson, and T. B. Jones, Stimulated electromagnetic emission (SEE) and anomalous HF wave absorption near electron gyroharmonics, *J. Geophys. Res., 99,* 6233-6246, 1994.

Thidé, B., H. Kopka, and P. Stubbe, Observations of stimulated scattering of a strong high-frequency radio wave in the ionosphere, *Phys. Rev. Lett., 49,* 1561-1564, 1982.

Thidé, B., H. Derblom, Å. Hedberg, H. Kopka, and P. Stubbe, Observations of stimulated electromagnetic emissions in ionospheric heating experiments, *Radio Sci., 18,* 851-859, 1983.

Thidé, B., Å. Hedberg, J. A. Fejer, and M. P. Sulzer, First observations of stimulated electromagnetic emission at Arecibo, *Geophys. Res. Lett., 16,* 369-372, 1989.

Tripathi, V. K., and C. S. Liu, *O* mode decay and upshifted electromagnetic emissions near cyclotron harmonics in the ionosphere, *J. Geophys. Res., 98,* 1719-1723, 1993.

Vas'kov, V. V., and A. V. Gurevich, Non-linear resonant instability of a plasma in the field of an ordinary electromagnetic wave, *Zh. Eksp. Teor. Fiz. 69,* 176-188, 1975. (*Sov. Phys. JETP,* Engl. Transl., *42,* 91-97, 1976.)

Vas'kov, V. V., and A. V. Gurevich, Resonance instability of small scale plasma perturbations (in Russian), *Zh. Eksp. Teor. Fiz., 73,* 923-936, 1977. (*Sov. Phys. JETP,* Engl. Transl., *46,* 487-494, 1978.)

Vas'kov, V. V., and A. V. Gurevich, Amplification of resonant instability and generation of wideband radio emission by high power radio waves incident on the ionosphere, *Geomagn. Aeron., 24,* 350-356, 1984.

Vas'kov, V. V., and G. S. Ivanov-Kholodiny, Acceleration of ionospheric plasma electrons by high-power radio wave under conditions of multiple electron gyro resonance, *Geomagn. Aeron., 31,* 839-844, 1991.

Villalon, E., Ionospheric electron acceleration by electromagnetic waves near regions of plasma resonances, *J. Geophys. Res., 94,* 2717-2720, 1989.

Weinstock, J., Enhanced airglow, electron acceleration, and parametric instabilities, *Radio Sci., 9,* 1085-1087, 1974.

F. Honary, Lancaster Communication Research Center, SECaM, Lancaster University, Lancaster LA1 4YR, England. (e-mail:F.Honary @lancaster.ac.uk)

T.B. Jones, T.R. Robinson, and A.J. Stocker, Department of Physics and Astronomy, Leicester University, Leicester, LE1 7RH, England. (e-mail:tbj@ion.le.ac.uk;txr@ion.le.ac.uk;sto@ion.le.ac.uk)

P. Stubbe, Max-Planck-Institut für Aeronomie, Postfach 20, D-37189 Katlenburg-Lindau, Germany. (e-mail:stubbe@linmpi.dnet.gwdg.de).

(Received February 6, 1995; revised June 21, 1995; accepted July 4, 1995.)